Molecular Pharmacology Fast Forward. Published on August 10, 2004 as doi:10.1124/mol.104.001008

Molecular dissection of butyrate action revealed the involvement of MAPK in CFTR biogenesis

Makoto Sugita, Hiroyasu Kongo, and Yoshiki Shiba

Department of Oral Physiology,
Graduate School of Biomedical Sciences,
Hiroshima University,
Kasumi 1-2-3, Minami-ku,
Hiroshima 734-8553, Japan

Molecular Pharmacology Fast Forward. Published on August 10, 2004 as DOI: 10.1124/mol.104.001008
This article has not been copyedited and formatted. The final version may differ from this version.

Running title: Involvement of MAPK in CFTR biogenesis

Address correspondence to;

Makoto Sugita

Department of Oral Physiology, Graduate School of Biomedical Sciences,

Hiroshima University,

Kasumi 1-2-3, Minami-ku, Hiroshima 734-8553, Japan

Tel: 81-82-257-5626, Fax: 81-82-257-5627

E-mail: sugisan@hiroshima-u.ac.jp

The number of text pages: 37

The number of tables: 0

The number of figures: 8

The number of references: 43

The number of words in the Abstract: 249

The number of words in the Introduction: 753

The number of words in the Discussion: 1337

Non-standard abbreviations used:

CFTR, cystic fibrosis transmembrane conductance regulator; GFP, green fluorescent protein; wt, wild type; DMEM, Dulbecco's modified Eagle's medium; NBD, nucleotide binding domain; MAPK, mitogen-activated protein kinase; ERK, extracellular signal-regulated kinase; ERAD, endoplasmic reticulum-associated degradation; ALLN, N-acetyl-leucyl-leucyl-norleucinal.

Abstract

Cystic fibrosis is caused by mutations in the cystic fibrosis transmembrane conductance regulator (CFTR) gene, which belongs to the superfamily of ABC transporters and uniquely possesses an additional large cytoplasmic domain (R domain). CFTR inefficiently folds by means of co- and post-translational interactions with the cytosolic chaperones as well as ER lumenal chaperones in the ER. Aberrant folding and defective trafficking of the CFTR protein, which functions as an apical membrane Cl^- channel, is the principal cause of cystic fibrosis. Recent data indicated that butyrate improves CFTR trafficking, in part, by regulating molecular chaperones. However, the precise mechanism of butyrate action remains elusive. In the present study, we examine the molecular aspect underlying the butyrate action in CFTR biogenesis, by evaluating the expression and localization of the GFP-tagged CFTR transgenes in Cos7 cells. Our data show that butyrate significantly promoted stability of the ER-located form of GFP-wt-CFTR, followed by an increase in the amount of plasma membrane GFP-wt-CFTR. In contrast, the expression of the R domain deletion mutant, GFP-ΔR-CFTR, was slightly increased by butyrate. The butyrate action on wt-CFTR expression was partially blocked by PD98059, a specific inhibitor of MAPKK/MEK which is the upstream activator of ERK/MAPK. Furthermore, activation of ERK/MAPK by coexpression of constitutively active MAPKK/MEK predominantly augmented the expression of wt-CFTR, but not of ΔR-CFTR, induced by butyrate. These data suggest that butyrate may facilitate the biogenesis and trafficking of wt-CFTR by requiring the presence of the R domain, and further involving active ERK/MAPK in its biogenesis.

Molecular Pharmacology Fast Forward. Published on August 10, 2004 as DOI: 10.1124/mol.104.001008
This article has not been copyedited and formatted. The final version may differ from this version.

Introduction

Cystic fibrosis is one of the most prevalent lethal genetic disorders among Caucasian population (Welsh and Smith, 1993). The CF gene encodes the cystic fibrosis transmembrane conductance regulator (CFTR), a cAMP-regulated Cl^- channel and conductance regulator, polarized to the apical membrane in numerous epithelia (Rommens et al., 1989). CFTR, a member of ABC transporter superfamily, is composed of two membrane-associated domains, each with six putative transmembrane segments, two nucleotide-binding domains (NBDs) and a large cytoplasmic R domain (Riordan et al., 1989). This complex, multidomain structure conceivably renders the posttranslational folding of wild-type CFTR inefficient. The majority (50-75%) of newly synthesized wild-type CFTR molecules remains incompletely folded and is degraded at endoplasmic reticulum (ER), whereas the remaining 25-50% undergoes an ATP-dependent conformational maturation and is exported to the cis/medial-Golgi, where its complex glycosylation occur (Lukacs et al., 1994; Ward and Kopito, 1994; Jensen et al., 1995). The most frequent mutation, deletion of phenylalanine at position 508 in the NBD1, increases the insufficiency of CFTR folding (to greater than 99%) and targets the core-glycosylated folding intermediate for degradation, predominantly via the ubiquitin-proteasome pathway at the ER (Ward and Kopito, 1994; Lukacs et al., 1993; Ward et al., 1995). Accordingly, negligible expression of ΔF508 CFTR could be detected at the cell surface (Kopito, 1999). However, the exciting finding that the ΔF508 CFTR Cl^- channel is partly functional both in the ER (Pasyk and Foskett, 1995) and after its reconstitution into planer lipid bilayers (Li et al., 1993) suggested that the CF phenotype could be alleviated by relocating the mutant CFTR from the ER to the plasma membrane by manipulating CFTR processing.

Butyrate, a short-chain fatty acid, is reported to function as a transcription activator, possibly via inhibition of histone deacetylase activity (D'Anna et al., 1980; Kruh, 1982), and modulate a variety of cellular events (Adam et al., 2003; Yang et al., 2001; Le Poul et al., 2003). Treatment with butyrate and the butyrate analog 4-

phenylbutyrate, which is approved for pharmaceutical use, corrects the ΔF508 CFTR trafficking defect and restores CFTR function at the plasma membrane (Cheng, et al., 1995; Rubenstein et al., 1997; Rubenstein and Zeitlin, 1998; Zeitlin et al., 2002). Wild-type CFTR, which is also folded inefficiently, could likewise be upregulated by this treatment (Kopito, 1999). Previous studies suggested that the enhancing effect of 4-phenylbutyrate on ΔF508 CFTR trafficking is elicited by decreased levels of heat shock cognate protein Hsc70, a constitutively expressed Hsp70 isoform (Rubenstein and Zeitlin, 2000). However, it is rather controversial whether butyrate and 4-phenylbutyrate influence ΔF508 CFTR folding or trafficking in addition to their effect on transcription, since the butyrate-induced overexpression of CFTR may simply overwhelm the ER's quality control (Cheng, et al., 1995; Gelman and Kopito, 2002). Thus, the molecular mechanisms of butyrate action on CFTR biogenesis remain elusive. Furthermore, butyrates appear to inhibit CFTR directly (Linsdell, 2001) and to suppress CFTR function indirectly by inhibiting Na-K-ATPases and Na-K-2Cl cotransporters, which are required for transepithelial salt transport (Moyer et al., 1999; Matthews et al., 1998). Thus, it is considered that the utility of butyrates as potential therapeutics may be limited by their inhibitory effects on the ion transporters in addition to the side effects elicited by the transcriptional activation of unidentified molecules. Nevertheless, identification of the specific targets of butyrate in CFTR biogenesis may lead to the possibility that CFTR processing can be manipulated by regulating their molecular functions. Thus, functional manipulation of the target molecules may enable us to perform the efficient CF treatment without side effects of butyrate.

To rationally develop therapeutic means to stimulate ΔF508 CFTR trafficking from the ER to the cell surface, it is first necessary to understand the mechanisms and pathways directing wild-type CFTR biogenesis and trafficking. In the present study, we examine the molecular aspect of the butyrate action on the biogenesis of CFTR, while comparing its action on the deletion mutant of the R domain, whose interaction with

NBD1 leads to the release of the Hsc70/Hdj-2 chaperone from CFTR during the critical step for CFTR biogenesis. By evaluating the expression and localization of the GFP-tagged CFTR transgenes in Cos7 cells, our data show that butyrate remarkably increased the amount of plasma membrane GFP-wt-CFTR, but not of GFP-ΔR-CFTR, with an aid of MAPK activity. Furthermore, the efficiency of the butyrate action on CFTR biogenesis, tightly depending on the cellular levels of active MAPK, suggests that MAPK activity may act as a rate-limiting step for the expression of mature CFTR, which is enhanced by butyrate treatment, and is mediated through the CFTR R domain.

Molecular Pharmacology Fast Forward. Published on August 10, 2004 as DOI: 10.1124/mol.104.001008
This article has not been copyedited and formatted. The final version may differ from this version.

Materials and Methods

Construction of mutants

The pEGFP-C1-CFTR mammalian expression vector, which allows fusion of GFP to the NH_2 terminus of CFTR, was kindly provided by Dr. Foskett. To construct the pEGFP-ΔR-CFTR mammalian expression vector, an AflII and SacI fragment from pTM1-CFTRΔR-S660A containing the C terminal region of was swapped with the wild-type cassette present in pEGFP-C1-CFTR. ΔF508-CFTR was made using a PCR-based mutagenesis technique. To construct the mutant ΔF508-CFTR, two rounds on PCR amplification were performed by KOD-plus- DNA polymerase (TOYOBO, Tokyo, Japan). By employing two flanking external primers which immediately flank single sites of BlpI and BstZ17I in CFTR, two overlapping fragments were generated in the first round of PCR amplification, using the internal mutagenic forward primer (5'-AGAAAATATCATCGGTGTTTCCTATGATGAATATAGATAC-3') with the 3'end external reverse primer and, in a separate reaction, using the internal mutagenic reverse primer (5'-CATAGGAAACACCGATGATATTTTCTTTAATGGTGCCAG-3') with the 5'end external forward primer. The two overlapping fragments generated in the first PCR were subjected to the second round of PCR amplification with external primers. The PCR-mutagenized cassette from the second step was swapped with the wild-type cassette present in pEGFP-C1-CFTR, using the unique restriction sites BlpI and BstZ17I. To insert a V5 tag between GFP and CFTR, the N terminus of CFTR was polymerase chain reaction (PCR) amplified, using the synthetic oligonucleotide primers which were designed to introduce a BspEI site and a V5 tag upstream of the CFTR initiation ATG codon (5'-TATTCCGGAGGTAAGCCTATCCCTAACCCTC TCCTCGGTCTCGATTCTACGATGCAGAGGTCGCCTCTGGAAAAG-3'), and to immediately flank a single BspEI site in CFTR. The BspEI-BspEI fragment was subcloned into the above clones to produce pEGFP-V5-CFTR, pEGFP-V5-ΔR-CFTR, and pEGFP-V5-ΔF508-CFTR. The PCR-amplified region was confirmed by sequencing.

Molecular Pharmacology Fast Forward. Published on August 10, 2004 as DOI: 10.1124/mol.104.001008
This article has not been copyedited and formatted. The final version may differ from this version.

Cells and CFTR expression

Cos7 cells were used for transfection and expression of wild-type and mutant CFTR proteins. The cells in 35 mm dishes were grown in DMEM (Gibco) supplemented with 10% FBS in 5% CO_2. They were transfected with pEGFP-CFTR for 12 h using the Lipofectamine reagent (Gibco), according to the manufacturer's instructions. Transfected Cos7 cells were then incubated for 12 h in the growing medium, followed by the further incubation in the presence or absence of 5 mM butyrate for 24 h. Fresh solution of butyrate were prepared immediately before use for each experiment.

SDS-PAGE and Western blotting

Cells were washed twice with 1ml PBS, solubilized in the buffer A (150 mM NaCl, 20 mM Tris-HCl (pH 8.0), 1% Triton X-100, 1 mM EDTA, 1 mM EGTA, 10% glycerol, 0.2 mM orthovanadate, and containing the Protease Inhibitor cocktail (SIGMA)), and spun at 14,000 *g* for 10 min to pellet insoluble materials. Aliquots of cell lysates were removed for SDS-PAGE analysis. Equal amounts of protein (5 μg) were separated on 2-15% SDS-polyacrylamide gradient gels (Daiichi), and transferred to nitrocellulose membranes. Membranes were blocked overnight at 4^{o}C in 5% non-fat dry milk in TBST, and incubated with primary antisera in the blocking solution, followed by horseradish peroxidase-conjugated secondary antibodies. Detection of immunoreactivity was performed with the enhanced chemiluminescence reagent (Perkin Elmer) and the medical X-ray film RX-U (Fuji Photo Film). Immunoblots, with multiple exposures, were quantified using Epscan transparency scanner and N.I.H. Image 1.63 software (developed by the National Institutes of Health and available at their web site).

Molecular Pharmacology Fast Forward. Published on August 10, 2004 as DOI: 10.1124/mol.104.001008
This article has not been copyedited and formatted. The final version may differ from this version.

Metabolic pulse-chase

The cells in 35 mm dishes were transfected with 1 μg of pEGFP-V5-CFTR, pEGFP-V5-ΔR-CFTR, or pEGFP-V5-ΔF508-CFTR, and incubated in the presence or absence of 5 mM butyrate for 24 h. The cells expressing the V5-tagged CFTR were starved in methionine/cysteine-free minimal essential media. After 1 h of methionine starvation, 200 μCi/ml Pro-mix L-[^{35}S] in vitro cell labeling mixture ([^{35}S]methionine/cysteine, Amersham Biosciences) was added, and cells were pulse-labeled for 30 min. The radioactive medium was then exchanged with cold, complete medium and cultured for various chase periods. Cells were solubilized in the buffer A at the time points indicated. Cell lysates were precleared with protein G-sepharose beads (Amersham), and the V5-tagged CFTR protein was immunoprecipitated using anti-V5 monoclonal antibody (Invitrogen) and protein G sepharose. The immunoprecipitates were washed extensively with the buffer B (150 mM NaCl, 20 mM Tris-HCl (pH 8.0), 1% Triton X-100, 1 mM EDTA, 1 mM EGTA) and fractionated by 2-15% gradient SDS-PAGE. Detection of radioactive bands was performed with BioMax TransScreen LE Intensifying Screen (Kodak) and BioMax MR films (Kodak). The bands were quantified using Epscan transparency scanner and N.I.H. Image 1.63 software.

Co-immunoprecipitation

The cells in 100 mm dishes were transfected with 4 μg of either pEGFP-V5-CFTR or pEGFP-V5-ΔR-CFTR for 12 h using the Lipofectamine reagent, incubated for 12 h in the growing medium, and followed by the further incubation in the presence or absence of 5 mM butyrate for 24 h. Cells were washed twice with 1ml PBS, solubilized in the buffer A, and spun at 14,000 *g* for 10 min to pellet insoluble materials. Aliquots of cell lysates (80 μg) were diluted with the buffer A to a final volume of 0.6 ml, and precleared with protein G-sepharose beads. The V5-tagged CFTR protein was immunoprecipitated using anti-V5 monoclonal antibody and protein

Molecular Pharmacology Fast Forward. Published on August 10, 2004 as DOI: 10.1124/mol.104.001008
This article has not been copyedited and formatted. The final version may differ from this version.

G sepharose beads. Beads were washed 3 times with the buffer B. Immunoprecipitates and co-immunoprecipitates were eluted from the Sepharose beads using the SDS sample buffer, and resolved by SDS-PAGE. Nitrocellurose blots of gels were probed with the antibodies to chaperone protein.

Statistical analysis

Results are presented as means $\pm$ S.E. of *n* observations. Unless noted otherwise, statistical significance was determined using unpaired Student's t test. *P* values <0.05 were considered statistically significant.

Visualizing the subcellular distribution of GFP fusion proteins in live cells

Transfected Cos7 cells were placed in a chamber (MI-IBX, Olympus), maintained in 5 % CO_2 at 37 ^{o}C, and observed under an inverted epifluorescence microscope (IX71, Olympus, Japan). The subcellular distribution of GFP-CFTR was visualized by the GFP fluorescence, excited using a Hg-lamp, and collected using a 510-525 nm band-pass filter. Time-lapse image processing was performed with MetaMorph software (Universal Imaging Co., West Chester, PA). Images were acquired every 15min with 8-s epifluorescence exposure, and stored in a computer.

Confocal imaging

Transfected Cos7 cells were washed twice with 1ml of PBS, fixed and permeabilized with 3.7% formaldehyde solution (1x PBS, 3.7% formaldehyde, 0.18% Triton X-100) for 10 min. Nonspecific binding sites were blocked with 1% BSA for 30 min. Cells were incubated with primary antisera, and then incubated with TRITC-conjugated secondary antibodies. Cells were observed under a confocal laser microscope (LSM410, Carl Zeiss, Germany). The subcellular distribution of GFP-CFTR was directly visualized by the GFP fluorescence, excited using a 488-nm laser line, and collected using a 510-525 nm band-pass filter. Fluorescence associated with

TRITC-labeled secondary antibodies was simultaneously excited using a 543-nm laser line and collected using a 570 nm long-pass filter. The fluorescent image and the differential interference contrast (DIC) image were imported into Adobe Photoshop version 7.0 for image processing and printing.

Materials

The following antibodies were used: HRP-conjugated goat polyclonal anti-GFP (600-103-215; Rockland), mouse monoclonal anti-HA (12CA5; Boehringer Mannheim), mouse monoclonal anti-phosphorylated ERK (sc-7383; Santa Cruz), rabbit polyclonal anti-Hsc70 (3095-100; BioVision), mouse monoclonal anti-V5 (R960-25; Invitrogen), mouse monoclonal anti-CFTR (clone24-1; R&D system), TRITC-conjugated goat anti-mouse IgG (RAF-011-2; EY laboratories), and HRP-conjugated anti-mouse IgG (sc-2005; Santa Cruz). The MEK inhibitor PD98059 and the p38 MAPK inhibitor SB203580 were purchased from Calbiochem. Wortmannin and butyrate were obtained from Sigma and Wako Pure Chemical, respectively.

Molecular Pharmacology Fast Forward. Published on August 10, 2004 as DOI: 10.1124/mol.104.001008
This article has not been copyedited and formatted. The final version may differ from this version.

Results

Effect of butyrate on GFP-CFTR expression

To elucidate the molecular aspect underlying the butyrate action on CFTR biogenesis, we evaluated the expression of green fluorescent protein (GFP) fused to the NH_2 terminus of either the wild-type or mutant CFTR, which allows us to directly visualize its subcellular distribution and to attain high sensitivity immunodetection, in Cos7 cells. Previous reports indicated that fusion of GFP to the NH_2 terminus of CFTR does not affect the trafficking and function of CFTR (Moyer et al., 1998). The immunoblot analysis showed that GFP-tagged wt-CFTR (GFP-wt-CFTR) appears as an immaturely glycosylated, ER-localized B form (~173 kDa) and a maturely glycosylated C from (~197 kDa)(Fig. 1AB). Thus, delivery of CFTR to the Golgi was detected by the conversion of the core-glycosylated B form to the complex glycosylated C form, diagnostic of processing by Golgi-associated mannosidases and glycosyltransferases leading to the addition of polylactosamine, as previously reported (Yoo et al., 2002). The electrophoresis mobility of GFP-wt-CFTR was appropriate for a chimera of GFP (~27 kDa) and full-length human CFTR (~145 kDa). Chronic butyrate treatment remarkably enhanced the steady-state levels of both the maturely glycosylated C form and the immaturely glycosylated B form of wt-CFTR in a dose-dependent fashion with the half-maximal activation constant of ~0.5 mM (Fig. 1AB). To compare with the previous reports (Moyer et al., 1999; Rubenstein et al., 1997), we selected the butyrate concentration of 5 mM and evaluated its action on CFTR biogenesis below. In contrast, the B form of the deletion mutant GFP-ΔR-CFTR, which lacks much of the R domain and replaces Ser^{660} with alanine (Rich et al., 1993), was detected as an approximately 15 kDa increase in electrophoresis mobility (~158 kDa)(Fig. 1B). The C form of GFP-ΔR-CFTR was also detectable with an apparent molecular mass of ~194 kDa (Fig. 1B). Compared with GFP-wt-CFTR, GFP-ΔR-CFTR expression was slightly increased by butyrate (Fig. 1BC). Time-lapse imaging revealed that butyrate treatment (5 mM) drastically induced the GFP-wt-CFTR expression around 12-27 h after the addition of

Molecular Pharmacology Fast Forward. Published on August 10, 2004 as DOI: 10.1124/mol.104.001008
This article has not been copyedited and formatted. The final version may differ from this version.

butyrate, and caused GFP-wt-CFTR to accumulate in the plasma membrane region (Fig. 2AC). In sharp contrast, the application of butyrate had little effect on the subcellular distribution of GFP-ΔR-CFTR, mainly located in the perinuclear region (Fig. 2AE). Since butyrate activates transcription from many viral promoters including the cytomegalovirus (CMV) promoter (Kruh, 1982; Shima et al., 1997), it is likely that the increased expression of GFP-wt-CFTR and GFP-ΔR-CFTR following butyrate treatment is partly attributable to activation of the CMV promoter driving its expression. Nevertheless, the butyrate-induced increase in CFTR expression may result from not only its transcriptional regulation but also its post-transcriptional regulation since GFP-wt-CFTR expression was predominantly enhanced by butyrate treatment, compared to GFP-ΔR-CFTR, with the identical efficiencies of the butyrate-activated transcription of wt- and ΔR-CFTRs, driven by the CMV promoter. These data may also imply that the R domain is involved in determining the efficiency of CFTR biogenesis.

To quantitatively compare the efficiency of maturation of CFTR from the band B to the band C forms, we evaluated the ratio of CFTR band C to CFTR band B in the presence or absence of butyrate. Although expression of GFP-ΔR-CFTR exhibited a significantly lower C/B ratio than its wt counterpart, the butyrate treatment had little effect on the C/B ratios of both wt-CFTR and ΔR-CFTR (Fig. 1D), suggesting that butyrate may modulate either the biogenesis or degradation of the ER-resident CFTR. To explore the biosynthetic steps of CFTR, which are affected by butyrate, the biological stability of GFP-wt-CFTR and GFP-ΔR-CFTR was determined upon inhibition of protein biosynthesis with cycloheximide, following the preincubation with butyrate. Cells were incubated in the presence of cycloheximide, and the remaining CFTR was measured with quantitative immunoblotting as a function of incubation time. Densitometry revealed that butyrate treatment did not significantly affect the proportions of the remaining C forms of wt-CFTR (Fig. 3AC) and ΔR-CFTR (Fig. 3BD). However, the disappearance rate of the ER-localized B form of wt-CFTR (the right panel in Fig. 3C), but not of ΔR-CFTR (the right panel of Fig. 3D), was

Molecular Pharmacology Fast Forward. Published on August 10, 2004 as DOI: 10.1124/mol.104.001008
This article has not been copyedited and formatted. The final version may differ from this version.

significantly slowed by butyrate treatment ($p<0.05$, $n=3$). Since the application of butyrate without cycloheximide had little effect on the C/B ratio, these results suggest that butyrate may stabilize the ER-localized B form of wt-CFTR. However, the amount of GFP-wt-CFTR in the ER following butyrate treatment is much higher than that in the control cells. This level of expression might simply overwhelm the ER's quality control mechanism. Thus, the reduced degradation by butyrate treatment might be secondary to its effect on transcription rather than a specific effect on CFTR folding or degradation. To address and argue against this, we attempted to manipulate the expression levels of CFTR by transfecting the various amounts of the expression plasmid, followed by a comparative study of CFTR degradation. The degradation of the C and B forms of wt-CFTR in the cells transfected with either 0.25 μg or 2 μg of the expression plasmid exhibited similar characteristics, compared to those in the cells transfected with 1 μg (Fig. 3ACE). Thus, butyrate treatment slowed the degradation rates of the ER-localized B form of wt-CFTR at the various expression levels. Although the identical levels of CFTR expression were observed in the control cells transfected with 2 μg of the expression plasmid, and in the butyrate-treated cells transfected with 0.25 μg, the degradation of the wt-CFTR B form was reduced in the butyrate-treated cells (Fig. 3E). Thus, these results suggest that the butyrate action plays a specific role in determining the rate of CFTR degradation, in addition to its effect on transcription. Since the degradation of ΔR-CFTR was less severely affected by butyrate treatment, these data suggest that butyrate promotes the stability of the B form of wt-CFTR in the ER, possibly in a R-domain-dependent manner.

To further characterize the butyrate action on CFTR biogenesis, we performed metabolic pulse-chase experiments as described previously (Gelman et al., 2002; Varga et al., 2004). In these experiments, we compared the amount of the newly synthesized B form, half-life, and its conversion to the C form among wt-CFTR, ΔR-CFTR, and ΔF508-CFTR as another control (Fig. 4). In either the butyrate-untreated cells or the butyrate-treated cells, the same levels of translation efficiency were observed among

Molecular Pharmacology Fast Forward. Published on August 10, 2004 as DOI: 10.1124/mol.104.001008
This article has not been copyedited and formatted. The final version may differ from this version.

the expressions of GFP-V5-wt-CFTR, GFP-V5-ΔR-CFTR, and GFP-V5-ΔF508-CFTR, judging from the amount of the pulse-labeled B form at t = 0 (Fig. 4A). Of note, butyrate treatment did not enhance translation efficiencies of wt-CFTR, ΔR-CFTR, and ΔF508-CFTR in Cos7 cells at this time point, 24h after the addition of butyrate (Fig. 4A). However, addition of butyrate significantly enhanced the stability of the B form of wt-CFTR ($p<0.05$), but not of ΔR-CFTR, and ΔF508-CFTR, without affecting the amounts of the converted C form (Fig. 4BCD). Early degradation of wt and mutant CFTR by proteasome has been described as a common feature of CFTR biogenesis (Jensen et al., 1995; Ward et al., 1995). To address whether a change in degradation rate is related to an effect on the ubiquitin-proteasome system, we investigated the effect of ALLN, a proteasome inhibitor, on protein half-life. In either butyrate-untreated cells or butyrate-treated cells, the addition of ALLN had little effect on the disappearance rate of the B forms of wt-CFTR (Fig. 4AB), suggesting that the butyrate-enhanced stability of the B form was not elicited by the proteasome inhibition. Therefore, in addition to proteasomes, other proteolytic systems might significantly contribute to ERAD for wt-CFTR (Jensen et al., 1995). Interestingly, addition of ALLN slightly and significantly slowed the disappearance of ΔR-CFTR, and ΔF508-CFTR in the butyrate-treated cells, but not in the butyrate-untreated cells (Fig. 4ACD), although during the chase without ALLN, the same levels of disappearance rate was observed between the butyrate-untreated and butyrate-treated cells. These results imply that butyrate may modulate the degradation of ΔR-CFTR, and ΔF508-CFTR, while slightly stimulating the proteasome-dependent ERAD, and inhibiting proteasome-independent ERAD at a certain equilibrium. Nevertheless, our results clearly demonstrate that butyrate remarkably enhanced the stability of the B form of wt-CFTR in sharp contrast with its effect on ΔR-CFTR, and ΔF508-CFTR.

MAPK activity determines the efficiency of the butyrate-induced expression of CFTR

Molecular Pharmacology Fast Forward. Published on August 10, 2004 as DOI: 10.1124/mol.104.001008
This article has not been copyedited and formatted. The final version may differ from this version.

To explore the molecular targets of butyrate, we have examined the effect of pharmacological reagents on the butyrate-induced increase in CFTR expression. Cells use a limited number of intracellular signaling pathways for a variety of cellular responses. One of those pathways is the classical mitogen-activated protein kinase (MAPK)/the extracellular signal-regulated kinase (ERK) cascade (Cobb and Goldsmith, 1995). In response to extracellular stimuli, MAP kinase kinase (MAPKK, also known as MEK), a direct activator for MAPK/ERK, becomes activated and then activates MAPK in the cytoplasm (Cobb and Goldsmith, 1995). Although the activated MAPK is translocated into the nucleus where it phosphorylates several nuclear targets, MAPK also phosphorylates the target molecules in the cytoplasm (Pierce et al., 2000). Although It is reported that not only does butyrate modulate MAPK activity in a cell type-dependent manner (Le Poul et al., 2003), but also is the endogeneous MAPK activity involved in determining and restricting the efficiency of the butyrate action (Yang et al., 2001), the involvement of MAPK either in CFTR biogenesis or in the butyrate action on its biogenesis remains elusive. To check whether MAPK regulates those steps, we examined the effect of PD98059, a specific inhibitor of MAPKK/MEK which is the upstream activator of ERK/MAPK. PD98059 (50 μM) partially inhibited the butyrate action on the enhancement of the steady-state levels of both the maturely glycosylated C form and immaturely glycosylated B form of wt-CFTR (Fig. 5AD)($p<0.05$, $n=3$). The application of PD98059 without butyrate treatment had no significant effect on the expression of the C form of wt-CFTR although it significantly ($p<0.05$) reduced the expression of the wt-CFTR B form (Fig. 5D). The biochemical data were supported by the results showing that the application of PD98059 prevented the cell-surface localization of CFTR, induced by butyrate treatment (Fig. 6). Importantly, the same levels of PD98059 sensitivity were observed between the expressions of CFTR and GFP-tagged CFTR (unpublished data), suggesting that the GFP fusion did not affect the role of MAPK. Compared with wt-CFTR, ΔR-CFTR expression was not significantly affected by the application of PD98059 either with or

Molecular Pharmacology Fast Forward. Published on August 10, 2004 as DOI: 10.1124/mol.104.001008
This article has not been copyedited and formatted. The final version may differ from this version.

without butyrate treatment (Fig. 5C). Inhibition of p38, another subfamily member of the MAPK superfamily, by a specific inhibitor SB203580 (10 μM) had no significant influence on the expressions of wt-CFTR and ΔR-CFTR either with or without butyrate (Fig. 5BC). Furthermore, inhibition of phosphatidylinositol 3-kinases, reported as a regulator of membrane trafficking of several channels and transporters (Kurashima et al., 1998), by wortmannin (200 nM) also had little effect on the steady-state levels of the B and C forms of wt-CFTR as well as ΔR-CFTR (Fig 5BC). Thus, our results imply that butyrate may improve the biogenesis of wt-CFTR, but not of ΔR-CFTR, by involving active ERK/MAPK. Since it is reported that Hsc70 specified by cochaperones significantly influences the efficiency of both CFTR biogenesis and degradation, we assessed the effect of butyrate and PD98059 on complex formation between CFTR and Hsc70. Although previous reports suggested that butyrate downregulated Hsc70 expression in the immortalized cystic fibrosis bronchiolar epithelial cell line IB3-1 (Rubenstein and Zeitlin, 2000), our results indicate that the expression level of Hsc70 was not affected by the treatment with butyrate and/or PD98059 in Cos7 cells (Fig. 5E). Hsc70 was coimmunoprecipitated with either wt-CFTR or ΔR-CFTR. The relative amount of Hsc70 coimmunoprecipitated with ΔR-CFTR was 2-fold greater than that with wt-CFTR (Fig. 5E). Butyrate treatment reduced the relative amount of Hsc70 coimmunoprecipitated with wt-CFTR as well as ΔR-CFTR (Fig. 5E). In the butyrate-treated cells, the addition of PD98059 further reduced the amount of Hsc70 coimmunoprecipitated with wt-CFTR (Fig. 5E), presumably by either stimulating their dissociation or preventing their association. In sharp contrast, the addition of PD98059 had little effect on complex formation between Hsc70 and ΔR-CFTR in the butyrate-treated cells (Fig. 5E). Since it is reported that Hsc70 associates with CFTR and facilitates the early steps in CFTR biogenesis, and its prolonged association with CFTR leads to degradation (Meacham et al., 1999), MAPK may transiently participate in regulating complex formation between Hsc70 and CFTR to facilitate the early steps in CFTR biogenesis, followed by the sequential second step

Molecular Pharmacology Fast Forward. Published on August 10, 2004 as DOI: 10.1124/mol.104.001008
This article has not been copyedited and formatted. The final version may differ from this version.

underlying the stabilization controlled by the butyrate-induced gene or the butyrate-regulated molecules.

To further clarify the involvement of MAPK in CFTR biogenesis, we coexpressed either wt-CFTR or ΔR-CFTR with the constitutively active mutant of MAPKK/MEK, which is a direct activator of ERK/MAPK. In the present study, LA-SDSE-MAPKK, in which Leu^{33}, Leu^{37}, Ser^{218}, and Ser^{222} were replaced by Ala, Ala, Asp, and Glu, respectively, was used as the constitutively active mutant (Fukuda et al., 1997). Coexpression of LA-SDSE-MAPKK induced an increase in the cellular levels of the active, phosphorylated ERK/MAPK (the lower panel in Fig. 7A), and predominantly augmented the expression of the B and C forms of CFTR, induced by butyrate treatment (the upper panel in Fig. 7A, and Fig. 7C), while the slight augmentation of CFTR expression was observed without butyrate treatment. These results appear to be consistent with the data of CFTR localization in the butyrate-treated cells showing that coexpression of LA-SDSE-MAPKK caused GFP-CFTR to accumulate in the cell-surface location in addition to a perinuclear location (Fig. 8). We also checked the effect of cotransfection of the dominant-negative construct, SASA-MAPKK, in which Ser^{218} and Ser^{222} were replaced by Ala (Gotoh et al., 1999). However, the cellular levels of active ERK/MAPKK were significantly reduced by CFTR transfection (Fig. 7A). Although PD98059 further reduced the active ERK/MAPK (Fig. 5D), cotransfection of SASA-MAPKK did not further decrease the cellular levels of active ERK/MAPKK in the CFTR-transfected cells. Therefore, cotransfection of SASA-MAPKK had little effect on CFTR expression (Fig. 7A). In sharp contrast with the effect on wt-CFTR, coexpression of LA-SDSE-MAPKK had little detectable influence on the expression of the B and C forms of ΔR-CFTR either with or without butyrate treatment (Fig. 7BD). Of note, neither butyrate treatment without LA-SDSE-MAPKK cotransfection nor the butyrate-induced overexpression of CFTR had significant effects on the endogenous levels of active ERK/MAPK in Cos7 cells (Fig. 7AB), suggesting that butyrate could facilitate CFTR biogenesis by

collaborating with endogenously activated MAPK, without further increasing active MAPK. However, the reducing and enhancing of MAPK activity resulted in an appearance of inhibitory and stimulatory effects on the butyrate-induced expression of CFTR, respectively. Thus, MAPK and the molecules either induced or regulated by butyrate may be synergistically, but not additively, involved in CFTR biogenesis or degradation. Taken together, our data suggest that the cellular MAPK activity may determine and restrict the efficiency of the expression of mature CFTR, which is enhanced by butyrate treatment, and is mediated through the CFTR R domain.

Molecular Pharmacology Fast Forward. Published on August 10, 2004 as DOI: 10.1124/mol.104.001008
This article has not been copyedited and formatted. The final version may differ from this version.

Discussion

Our data show that butyrate remarkably increased the expression of the plasma-membrane-localized GFP-wt-CFTR, whereas GFP-ΔR-CFTR expression was slightly increased by butyrate. Although there was a variability in the levels of the butyrate-induced augmentation of the ΔR-CFTR expression, presumably by means of the cellular expression levels of the molecules involved in the butyrate action and CFTR biogenesis, butyrate caused the more significant increase in the wt-CFTR expression, compared to the ΔR-CFTR expression. It is controversial whether butyrate and the butyrate analogue 4-phenyl butyrate affect CFTR folding and trafficking in addition to their effect on transcription (Gelman and Kopito, 2002; Cheng et al., 1995; Rubenstein et al., 1997). However, our data indicate that the influence of butyrate on CFTR biogenesis is not simply caused by transcriptional regulation, and thus overwhelming of the ER's quality control. First, although the identical efficiencies of the CMV promoter-driven transcription and translation of wt-CFTR and ΔR-CFTR were observed in metabolic pulse-chase experiments, butyrate treatment predominantly enhanced GFP-wt-CFTR expression in comparison with GFP-ΔR-CFTR. Second, both half-life studies and the cycloheximide application revealed that butyrate treatment enhanced CFTR expression by promoting stability of the ER-located B form of wt-CFTR, but not of ΔR-CFTR, suggesting that the presence of the R domain is required for CFTR to facilitate its biogenesis enhanced by butyrate treatment. Third, when the identical levels of wt-CFTR expression were induced in the control cells and in the butyrate-treated cells, the degradation of the B form was remarkably slowed in the butyrate-treated cells in comparison with the control cells. Therefore, butyrate treatment may elicit the specific post-transcriptional regulation of CFTR folding or degradation, in addition to its transcriptional regulation, leading to an increase in the expression of plasma membrane CFTR.

Wild-type CFTR is predominantly found as a complex-glycosylated form in the post-ER membrane including the plasma membrane, while ΔF508-CFTR is found as an

Molecular Pharmacology Fast Forward. Published on August 10, 2004 as DOI: 10.1124/mol.104.001008
This article has not been copyedited and formatted. The final version may differ from this version.

immature, core-glycosylated form localized to the ER membrane. The R domain deletion mutant possessed intermediate characteristics of the C/B ratio and the subcellular distribution. It is reported that CFTR maturation can utilize the non-conventional pathway, including the COPII export machinery, whereby the protein is first likely to be transported to distal Golgi compartment and/or the endosomal system prior to retrieval to earlier Golgi compartments for oligosaccharide processing to the complex form (Yoo et al., 2002). The lower C/B ratio observed in ΔR-CFTR expression than the wild-type counterpart suggests that wt-CFTR may more efficiently interact with trafficking components such as the COPII export machinery than does ΔR-CFTR to divert CFTR away from the ER quality control systems that normally scan the ER for misfolded CFTR. Nevertheless, butyrate treatment had little detectable influence on the C/B ratios of both wt-CFTR and ΔR-CFTR, and the conversion of the B form to the C form in metabolic pulse-chase experiments, importantly suggesting that the molecular targets of butyrate may exist in the pre-Golgi compartment. The increased stability of the ER-located B form, observed in wt-CFTR expression, support that this is the case.

The relative levels of the cellular protein folding and surveillance machinery dictate the time given to CFTR biogenic intermediates to reach the native state and thus influence the overall efficiency of its maturation. Several molecular chaperones have been suggested to facilitate CFTR biogenesis and maturation. Cytosolic chaperones Hsp70, Hsc70, Hdj-2 and Hsp90, as well as the ER lumenal chaperone calnexin transiently associate with CFTR in the ER, and their dissociation coincides with CFTR maturation (Kopito, 1999; Loo et al., 1998; Meacham et al., 1999). Particularly, the cellular levels of cochaperones, such as CHIP and Hdj2, that specify Hsc70 function seem to directly influence the efficiencies of both CFTR biogenesis and CFTR degradation (Meacham et al., 1999; Meacham et al., 2001). The present studies suggest that the complex formation between Hsc70 and CFTR is affected by butyrate and ERK/MAPKK activity. However, the CFTR expression, enhanced by butyrate and

augmented by active MAPK, may not be simply elicited by the dissociation of Hsc70 at a single step. Rather, MAPK might regulate the complex formation between Hsc70 and CFTR to facilitate the early steps in CFTR biogenesis, followed by the sequential step where the butyrate-induced genes or the butyrate-regulated molecules could control the CFTR stability, while releasing the Hsc70 complexes from CFTR. During the sequential steps of the synthesis and cotranslational folding of CFTR, the Hdj-2/Hsc70 chaperone pair participates in either promoting NBD1 folding or stabilizing it (Meacham et al., 1999). The synthesized R domain then interacts with the N-terminal half of CFTR in a manner that reduces Hdj-2 binding, presumably with NBD1 and the R domain forming a complex which buries some of the binding sites on CFTR for Hdj-2 (Meacham et al., 1999). The stabilization of NBD1-R domain interactions, which leads to the release of most of the Hdj-2 from CFTR, appears to involve the formation of an MSD1-MSD2 complex within the ER membrane (Meacham et al., 1999; Ostedgaard et al., 1997). Thus, the assembly defect, elicited by the deletion of the R domain in the present study, might cause chaperone-binding sites on CFTR to remain exposed, and contribute to the diversion of ΔR-CFTR from its biogenic pathway to degradation. Importantly, our comparative data exploring the biogenesis of wt-CFTR and ΔR-CFTR suggest that butyrate might act on this step by involving MAPK activity since the deletion of the R domain attenuated the butyrate action of increasing the stability of the B form, and the cooperative action of MAPK with butyrate in facilitating CFTR biogenesis. Furthermore, judging from that inhibition of MAPK activity by PD98059, and its activation by LA-SDSE-MAPKK coexpression caused the butyrate action to suppress and to augment, respectively, our results suggest that endogenous MAPK activity may determine the efficiency of the butyrate action on CFTR expression. Thus, MAPK may function as a rate-limiting step for the butyrate action on CFTR biogenesis, requiring the presence of the R domain for CFTR to facilitate its biogenesis. Therefore, the manipulation of the cellular MAPK activity might be of critical relevance for controlling the expression levels of the plasma-

Molecular Pharmacology Fast Forward. Published on August 10, 2004 as DOI: 10.1124/mol.104.001008
This article has not been copyedited and formatted. The final version may differ from this version.

membrane-located CFTR. Manifestation of the butyrate action may require expression of and CFTR interaction with another molecules(s), although neither the nature of this interaction nor the other molecule(s) are known. Butyrate-induced genes might be regulated by MAPK phosphorylation to facilitate CFTR biogenesis. Alternatively, the MAPK-induced genes might undergo the functional regulation by butyrate. In the present study, our results suggest an important role for the R domain in contributing to manifestation of the efficient butyrate action and the MAPK-regulated augmentation of CFTR expression, since its deletion attenuates those effects. Thus, the R domain may play a key role in the regulatory interaction.

Deletion of Phe^{508} reduces the efficiency with which CFTR fold, leading to alter the protein's interaction with the quality control system in the ER (Sharma et al., 2001; Gelman et al., 2002). Although this mutation also alters the kinetics of CFTR gating (Haws et al., 1996) and its stability as a cell surface glycoprotein (Sharma et al., 2001; Heda et al., 2001), the ΔF508-CFTR Cl^- channel is partly functional. Therefore, it is suggested that the first step for the CF therapy with this mutation is to rescue the ΔF508-CFTR mislocalization in the ER. The previous study revealed that complexes between Hsc70/Hdj-2 with immature ΔF508-CFTR were ~2 fold more abundant than similar complexes with CFTR (Meacham et al., 1999), implying that ΔF508-CFTR has more difficulty than CFTR in progressing to a point in its folding pathway, where it buries binding sites for Hdj-2 and Hsc70, with an aid of the R domain. In this case, the primary folding defect, derived from the ΔF508-NBD1, may elicit the inadequate exposure of those binding sites, whereas the R domain might be intact. Further studies will be required to clarify the direct molecular targets of butyrate and MAPK to facilitate CFTR biogenesis by involving the R domain because the specific engineering of those molecular functions may enable the efficient CF treatment for trafficking mutants without side effects of butyrate, and thus for the patients who use such a therapy throughout a life.

Molecular Pharmacology Fast Forward. Published on August 10, 2004 as DOI: 10.1124/mol.104.001008
This article has not been copyedited and formatted. The final version may differ from this version.

Acknowledgements

We thank Dr. K. Foskett for providing pEGFP-CFTR, Dr. M. Welsh for CFTRΔR-S660A, and Dr. E. Nishida for LD-SDSE-MAPKK and SASA-MAPKK. We sincerely thank the members in Radioisotope Research Facility, Hiroshima University, for supporting the RI research.

References

Adam E, Quivy V, Bex F, Chariot A, Collette Y, Vanhulle C, Schoonbroodt S, Goffin V, Nguyen TL, Gloire G, et al. (2003) Potentiation of tumor necrosis factor-induced NF-kappa B activation by deacetylase inhibitors is associated with a delayed cytoplasmic reappearance of I kappa B alpha. *Mol Cell Biol* **23**:6200-6209.

Cheng SH, Fang SL, Zabner J, Marshall J, Piraino S, Schiavi SC, Jefferson DM, Welsh MJ and Smith AE (1995) Functional activation of the cystic fibrosis trafficking mutant DF508-CFTR by overexpression. *Am J Physiol* **268**:L615-L624.

Cobb MH and Goldsmith EJ (1995) How MAP kinases are regulated. *J Biol Chem* **270**:14843-14846.

D'Anna JA, Tobey RA and Gurley LR (1980) Concentration-dependent effects of sodium butyrate in Chinese hamster cells: cell-cycle progression, inner-histone acetylation, histone H1 dephosphorylation, and induction of an H1-like protein. *Biochemistry* **19**:2656-2671.

Fukuda M, Gotoh I, Adachi M, Gotoh Y and Nishida E (1997) A novel regulatory mechanism in the mitogen-activated protein (MAP) kinase cascade. *J Biol Chem* **272**:32642-32648.

Gelman MS, Kannegaard ES and Kopito RR (2002) A principal role for the proteasome in endoplasmic reticulum-associated degradation of misfolded intracellular cystic fibrosis transmembrane conductance regulator. *J Biol Chem* **277**:11709-11714.

Gelman MS and Kopito RR (2002) Rescuing protein conformation: prospects for pharmacological therapy in cystic fibrosis. *J Clin Invest* **110**:1591-1597.

Gotoh I, Fukuda M, Adachi M and Nishida E (1999) Control of the cell morphology and the S phase entry by mitogen-activated protein kinase kinase. *J Biol Chem* **274**:11874-11880.

Haws CM, Nepomuceno IB, Krouse ME, Wakelee H, Law T, Xia Y, Nguyen H and Wine JJ (1996) ΔF508-CFTR channels: kinetics, activation, by forskolin, and potentiation by xanthines. *Am J Physiol* **270**:C1544-C1555.

Heda GD, Tanwani M and Marino CR (2001) The ΔF508 mutation shortens the biochemical half-life of plasma membrane CFTR in polarized epithelial cells. *Am J Physiol* **280**:C166-C174.

Jensen TJ, Loo MA, Pind S, Williams DB, Goldberg AL and Riordan JR (1995) Multiple proteolytic systems, including the proteasome, contribute to CFTR processing. *Cell* **83**:129-135.

Kopito RR (1999) Biosynthesis and degradation of CFTR. *Physiol Rev* **79**(Suppl.):S167-S173.

Kruh J (1982) Effect of sodium butyrate, a new pharmacological agents, on cells in culture. *Mol Cell Biochem* **12**:65-82.

Kurashima K, Szabo EZ, Lukacs G, Orlowski J and Grinstein S (1998) Endosomal recycling of the Na^+/H^+ exchanger NHE isoform is regulated by the phosphatidylinositol 3-kinase pathway. *J Biol Chem* **273**:20828-20836.

Le Poul E, Loison C, Struyf S, Springael JY, Lannoy V, Decobecq ME, Brezillon S, Dupriez V, Vassart G, Van Damme J, et al. (2003) Functional characterization of human receptors for short chain fatty acids and their role in polymorphonuclear cell activation. *J Biol Chem* **278**:25481-25489.

Li C, Ramjeesingh M, Reyes E, Jensen T, Chang X, Rommens JM and Bear CE **(**1993) The cystic fibrosis mutation (ΔF508) does not influence the chloride channel activity of CFTR. *Nat. Genet* **3**:311-316.

Linsdell P (2001) Direct block of the cystic fibrosis transmembrane conductance regulator Cl^- channel by butyrate and phenylbutyrate. *Eur J Pharmacol* **411**:255-260.

Loo MA, Jensen TJ, Cui L, Hou Y, Chang XB and Riordan JR (1998) Perturbation of Hsp90 interaction with nascent CFTR prevents its maturation and accelerates its degradation by the proteasome. *EMBO J* **17**:6879-6887.

Lukacs GL, Chang XB, Bear C, Kartner N, Mohamed A, Riordan JR and Grinstein S (1993) The ΔF508 mutation decreases the stability of cystic fibrosis transmembrane

conductance regulator in the plasma membrane. Determination of functional half-lives on transfected cells. *J Biol Chem* **268**:21592-21598.

Lukacs GL, Mohamed A, Kartner N, Chang XB, Riordan JR and Grinstein S (1994) Conformational maturation of CFTR but not its mutant counterpart (DF508) occurs in the endoplasmic reticulum and requires ATP. *EMBO J* **13**:6076-6086.

Matthews JB, Hassan I, Meng S, Archer SY, Hrnjez BJ and Hodin RA (1998) Na-K-2Cl cotransporter gene expression and function during enterocyte differentiation. Modulation of Cl^- secretory capacity by butyrate. *J Clin Invest* **101**: 2072-2079.

Meacham GC, Lu Z, King S, Sorscher E, Tousson A and Cyr DM (1999) The Hdj-2/Hsc70 chaperone pair facilitates early steps in CFTR biogenesis. *EMBO J* **18**:1492-1505.

Meacham GC, Patterson C, Zhang W, Younger JM and Cyr DM (2001) The Hsc70 co-chaperone CHIP targets immature CFTR for proteasomal degradation. *Nat Cell Biol* **3**:100-105.

Moyer BD, Loffing J, Schwiebert EM, Loffing-Cueni D, Halpin PA, Karlson KH, Ismailov II, Guggino WB, Langford GM and Stanton BA (1998) Membrane trafficking of the cystic fibrosis gene products, cystic fibrosis transmembrane conductance regulator, tagged with green fluorescent protein in Madin-Darby canine kidney cells. *J Biol Chem* **273**:21759-21768.

Moyer BD, Loffing-Cueni D, Loffing J, Reynolds D and Stanton BA (1999) Butyrate increases apical membrane CFTR but reduces chloride secretion in MDCK cells. *Am J Physiol* **277**:F271-F276.

Ostedgaard LS, Rich DP, DeBerg LG and Welsh MJ (1997) Association of domains within the cystic fibrosis transmembrane conductance regulator. *Biochemistry* **36**:1287-1294.

Pasyk EA and Foskett JK (1995) Mutant (ΔF508) cystic fibrosis transmembrane conductance regulator Cl^- channel is functional when retained in endoplasmic reticulum of mammalian cells. *J Biol Chem* **270**:12347-12350.

Pierce KL, Maudsley S, Daaka Y, Luttrell LM and Lefkowitz RJ **(**2000) Role of endocytosis in the activation of the extracellular signal-regulated kinase cascade by sequestering and nonsequestering G protein-coupled receptors. *Proc Natl Acad Sci USA* **97**:1489-1494.

Rich DP, Berger HA, Cheng SH, Travis SM, Saxena M, Smith AE and Welsh MJ (1993) Regulation of the cystic fibrosis transmembrane conductance regulator Cl^- channel by negative charge in the R domain. *J Biol Chem* **268**:20259-20267.

Riordan JR, Rommens JM, Kerem B, Alon N, Rozmahel R, Grzelczak Z, Zielenski J, Lok S, Plavsic N, Chou JL, et al. (1989) Identification of the cystic fibrosis gene: cloning and characterization of complementary DNA. *Science* **245**:1066-1073.

Rommens JM, Iannuzzi MC, Kerem B, Drumm ML, Melmer G, Dean M, Rozmahel R, Cole JL, Kennedy D, Hidaka N, et al. (1989) Identification of the cystic fibrosis gene: chromosome walking and jumping. *Science* **245**:1059-1065.

Rubenstein RC, Egan ME and Zeitlin PL (1997) In vitro pharmacologic restoration of CFTR-mediated chloride transport with sodium 4-phenylbutyrate in cystic fibrosis epithelial cells containing ΔF508-CFTR. *J Clin Invest* **100**:2457-2465.

Rubenstein RC and Zeitlin PL (1998) A pilot clinical trial of sodium 4-phenylbutyrate (buphenyl) in ΔF508-homozygous cystic fibrosis patients: evidence of restoration of nasal epithelial CFTR function. *Am J Resp Crit Care Med* **157**:484-490.

Rubenstein RC and Zeitlin PL (2000) Sodium 4-phenylbutyrate downregulates Hsc70: implication for intracellular trafficking of ΔF508-CFTR. *Am J Physiol* **278**:C259-C267.

Sharma M, Benharouga M, Hu W and Lukacs GL **(**2001) Conformational and temperature-sensitive stability defects of the ΔF508 cystic fibrosis transmembrane conductance regulator in post-endoplasmic reticulum compartments. *J Biol Chem* **276**:8942-8950.

Shima DK, Haldar K, Pepperkok R, Watson R and Warren G (1997) Partitioning of the Golgi apparatus during mitosis in living HeLa cells. *J Cell Biol* **137**:1211-1228.

Varga K, Jurkuvenaite A, Wakefield J, Hong JS, Guimbellot JS, Venglarik CJ, Niraj A, Mazur M, Sorscher EJ, Collawn JF and Bebok Z (2004) Efficient intracellular processing of the endogenous cystic fibrosis transmembrane conductance regulator in epithelial cell lines. *J Biol Chem* **279**:22578-22584.

Ward CL and Kopito RR (1994) Intracellular turnover of cystic fibrosis transmembrane conductance regulator. Inefficient processing and rapid degradation of wild-type and mutant proteins. *J Biol Chem* **269**:25710-25718.

Ward CL, Omura S and Kopito RR (1995) Degradation of CFTR by the ubiquitin-proteasome pathway. *Cell* **83**:121-127.

Welsh MJ and Smith AE (1993) Molecular mechanism of CFTR chloride channel dysfunction in cystic fibrosis. *Cell* **73**:1251-1254.

Yang J, Kawai Y, Hanson RW and Arinze IJ (2001) Sodium butyrate induces transcription from the G alpha(i2) gene promoter through multiple Sp1 sites in the promoter and by activating the MEK-ERK signal transduction pathway. *J Biol Chem* **276**:25742-25752.

Yoo J-S, Moyer BD, Bannykh S, Yoo H-M, Riordan JR and Balch WE 2002. Non-conventional trafficking of the cystic fibrosis transmembrane conductance regulator through the early secretory pathway. *J Biol Chem* **277**:11401-11409.

Zeitlin PL, Diener-West M, Rubenstein RC, Boyle MP, Lee CKK and Brass-Ernst L (2002) Evidence of CFTR function in cystic fibrosis after systemic administration of 4-phenylbutyrate. *Mol Ther* **6**:119-126.

Molecular Pharmacology Fast Forward. Published on August 10, 2004 as DOI: 10.1124/mol.104.001008
This article has not been copyedited and formatted. The final version may differ from this version.

Footnotes

This research was supported by a Grant-in-Aid for Scientific Research from the Ministry of Education, Science, Sports and Culture of Japan (11771137, 13771094, and 15791059 to M.S.).

Molecular Pharmacology Fast Forward. Published on August 10, 2004 as DOI: 10.1124/mol.104.001008
This article has not been copyedited and formatted. The final version may differ from this version.

Legends for figures

Figure 1: **Effect of butyrate on the expression and maturation of GFP-wt-CFTR and GFP-ΔR-CFTR.** (**A**) The expression of GFP-wt-CFTR in transiently transfected Cos7 cells and non-transfected cells (control) was monitored with immunoblotting 24 h after the addition of various concentrations of butyrate. B and C denote the immaturely glycosylated ER and maturely glycosylated plasma-membrane forms of CFTR, respectively. (**B**) The expression of GFP-wt-CFTR and GFP-ΔR-CFTR in transiently transfected Cos7 cells and non-transfected cells (control) was monitored with immunoblotting using an anti-GFP antibody. Cos7 cells, transfected with 1 μg of GFP-wt-CFTR or GFP-ΔR-CFTR expression plasmid, were incubated for 24 h in the presence or absence of 5 mM butyrate. (**C**) Relative intensities of GFP-CFTR bands were quantified. The complex glycosylated C (white columns) and the core-glycosylated B (black columns) forms of either GFP-wt-CFTR or GFP-ΔR-CFTR expressed in Cos7 cells were calculated from densitometry of immunoblots shown on (B). The amounts of the B and C forms in Cos7 cells without butyrate treatment were set to 1, and the relative amounts of those forms with butyrate treatment were quantified. The data are expressed as the mean $\pm$ SEM of 11 and 6 independent experiments for wt-CFTR and ΔR-CFTR, respectively. (**D**) Comparison of the ratio of CFTR band C to band B in the presence and absence of butyrate. CFTR maturation from the immature band B to the mature band C form was evaluated from densitometry of immunoblots. The data are expressed as the mean $\pm$ SEM of 11 and 6 independent experiments for wt-CFTR and ΔR-CFTR, respectively.

Figure 2: **Effect of butyrate on the subcellular distribution of GFP-wt-CFTR and GFP-ΔR-CFTR in Cos7 cells.** (**A**) By confocal imaging, the subcellular distribution of GFP-wt-CFTR and GFP-ΔR-CFTR, transiently expressed in Cos7 cells in the absence (control) or presence of 5 mM butyrate, was directly visualized by the GFP fluorescence (top) 24 h after the addition of butyrate. DIC images (bottom) were also

revealed. (**B-D**) Visualization of the subcellular distribution of GFP-wt-CFTR and GFP-ΔR-CFTR in the live cells treated with or without butyrate. The sequential images, taken at the indicated time points (hour) after the addition of butyrate, are shown.

Figure 3: **Effect of butyrate on stability of the wt-CFTR and ΔR-CFTR cellular pool.** (**A**) Representative immunoblots showing the disappearance of the B and C forms of GFP-wt-CFTR, monitored in the presence of cycloheximide. Cells were transfected with 1 μg of the GFP-wt-CFTR expression plasmid, incubated with or without butyrate treatment for 24 h, and harvested at the indicated time points after the addition of cycloheximide (25 μg/ml). Cells were solubilized and equal amounts of protein (5 μg) were immunoblotted with an anti-GFP antibody. (**B**) Representative immunoblots showing the disappearance of the B and C forms of GFP-ΔR-CFTR, monitored in the presence of cycloheximide. Cells were transfected with 1 μg of the GFP-ΔR-CFTR expression plasmid, and analyzed as (A). (**C**) Relative intensities of the C and B forms of GFP-wt-CFTR, monitored in the presence of cycloheximide. The complex glycosylated C (left) and the core-glycosylated B (right) forms of GFP-wt-CFTR persisting in the cells were calculated from densitometry of immunoblots shown on (A). The initial amounts of the B and C forms either with (open triangles) or without (closed circles) butyrate treatment were set to 1, and the relative amounts of those forms at the indicated time points were quantified. The data are expressed as the mean $\pm$ SEM of three independent experiments. (**D**) Relative intensities of the C and B forms of GFP-ΔR-CFTR, monitored in the presence of cycloheximide. The C (left) and the B (right) forms of GFP-ΔR-CFTR persisting in the cells were calculated from densitometry of immunoblots shown on (B). The relative amounts of those forms either with (open triangles) or without (closed circles) butyrate treatment at the indicated time points were quantified as (C). (**E**) Representative immunoblots showing the relation between the expression levels and the degradation rates of GFP-wt-CFTR in the presence and absence of butyrate. Cells were transfected with either 0.25 μg or 2μg of the GFP-wt-

Molecular Pharmacology Fast Forward. Published on August 10, 2004 as DOI: 10.1124/mol.104.001008
This article has not been copyedited and formatted. The final version may differ from this version.

CFTR expression plasmid, and analyzed as (A). The representative data from three independent experiments were shown.

Figure 4: **Pulse-chase analysis of degradation and maturation of wild-type and mutant CFTR.** (**A**) Representative pulse-chase data showing degradation and maturation of wild-type and mutant CFTR proteins in Cos7 cells treated with or without butyrate, and monitored in the presence or absence of ALLN. Cos7 cells were transfected with 1 μg of the expression plasmids of GFP-V5-wt-CFTR, GFP-V5-ΔR-CFTR, or GFP-V5-ΔF508-CFTR, and incubated for 24 h in the presence or absence of 5 mM butyrate. The cells were labeled with [^{35}S]methionine/cysteine and chased for the indicated time intervals in the presence or absence of 50 μM ALLN. Cells were then solubilized, and lysates were immunoprecipitated with anti-V5 antibody. The immunoprecipitated CFTR proteins were resolved by SDS-PAGE. (**B**) Quantification of the B and C forms of pulse-labeled GFP-V5-wt-CFTR. The C and B forms of GFP-wt-CFTR persisting in the cells were calculated from densitometry of radioactive bands shown on (A). The initial total amounts of the B and C forms after a 30-min pulse were set to 1, and the relative amounts of those forms at the indicated time points were quantified. The data are expressed as the mean $\pm$ SEM of two independent experiments.

In the left panel, the disappearance rates of the B form in Cos7 cells treated with butyrate (closed triangles) or without butyrate (closed circles) were calculated. Formations of the C form in Cos7 cells treated with butyrate (open triangles) and without butyrate (open circles) were also denoted. In the middle panel, disappearance of the B form in Cos7 cells, which were not treated with butyrate, was chased with ALLN (open squares) or without ALLN (closed circles) and compared. In the right panel, disappearance of the B form in the butyrate-treated Cos7 cells was chased with ALLN (open squares) or without ALLN (closed triangles) and compared. (**C**) Quantification of the B form of pulse-labeled GFP-V5-ΔR-CFTR. Since the C form of

Molecular Pharmacology Fast Forward. Published on August 10, 2004 as DOI: 10.1124/mol.104.001008
This article has not been copyedited and formatted. The final version may differ from this version.

pulse-labeled GFP-V5-ΔR-CFTR was not clearly observed during the chase periods, the only B form of GFP-V5-ΔR-CFTR persisting in the cells was calculated from densitometry of radioactive bands shown on (A). Thus, the initial total amounts of the B form after a 30-min pulse were set to 1, and the relative amounts at the indicated time points were quantified. The data are expressed as the mean ± SEM of two independent experiments.

In the left panel, the disappearance rates of the B form of GFP-V5-ΔR-CFTR in Cos7 cells treated with butyrate (closed triangles) or without butyrate (closed circles) were calculated. In the middle panel, disappearance of the B form of GFP-V5-ΔR-CFTR in Cos7 cells, which were not treated with butyrate, was chased with ALLN (open squares) or without ALLN (closed circles) and compared. In the right panel, disappearance of the B form of GFP-V5-ΔR-CFTR in butyrate-treated Cos7 cells was chased with ALLN (open squares) or without ALLN (closed triangles) and compared. (**D**) Quantification of the B form of pulse-labeled GFP-V5-ΔF508-CFTR. Since the C form of pulse-labeled GFP-V5-ΔF508-CFTR was not clearly observed during the chase periods, the only B form of GFP-V5-ΔF508-CFTR persisting in the cells was calculated from densitometry of radioactive bands shown on (A) and compared as (C).

Figure 5: **Effect of PD98059, SB203580 and wortmannin on the expression of GFP-wt-CFTR and GFP-ΔR-CFTR in Cos7 cells exposed to butyrate.** (**A**) The expression of GFP-wt-CFTR in transiently transfected Cos7 cells was monitored in the presence of PD98059 and/or butyrate with immunoblotting using an anti-GFP antibody. Cos7 cells, transfected with 1 μg of the GFP-wt-CFTR expression plasmid, were harvested at the indicated time points after the addition of PD98059 (50 μM) and/or butyrate (5 mM). (**B**) The effect of SB203580 and wortmannin on GFP-wt-CFTR expression revealed by immunoblotting. Cos7 cells, transiently expressing GFP-wt-CFTR, were harvested 24 h after the addition of SB203580 (10 μM) or wortmannin (200 nM) either with or without butyrate treatment, and were compared to the control

Molecular Pharmacology Fast Forward. Published on August 10, 2004 as DOI: 10.1124/mol.104.001008
This article has not been copyedited and formatted. The final version may differ from this version.

cells without treatment of SB203580 and wortmannin. (**C**) The effect of PD98059, SB203580 and wortmannin on GFP-ΔR-CFTR expression revealed by immunoblotting. Cos7 cells, transiently expressing GFP-ΔR-CFTR, were harvested 24 h after the addition of PD98059, SB203580 or wortmannin either with or without butyrate treatment. (**D**) Relative intensities of the C and B forms of GFP-wt-CFTR, monitored in the presence of PD98059 and/or butyrate. The complex glycosylated C (white columns) and the core-glycosylated B (black columns) forms of GFP-wt-CFTR expressed in the cells were calculated from densitometry of immunoblots. The amounts of the B and C forms with butyrate treatment were set to 1, and the relative amounts of those forms in the presence of PD98059 were quantified. The data are expressed as the mean ± SEM of three independent experiments. In the lower panel, the cellular levels of the phosphorylated, active form of ERK/MAPK in the various experimental conditions were evaluated using anti-phosphorylated ERK mAb. (**E**) The effect of butyrate and PD98059 on complex formation between CFTR and Hsc70. Cos7 cells were transiently transfected with the expression plasmid encoding GFP-V5-wt-CFTR, or GFP-V5-ΔR-CFTR, and incubated for 24 h in the presence of butyrate and/or PD98059. Cells were solubilized, and V5-tagged CFTR and associated proteins in the lysates were immunoprecipitated with anti-V5 antibody. The components of V5-CFTR immune complexes were then probed by the western blot using anti-V5 (the upper blot) and anti-Hsc70 (the middle blot). The amounts of immunoprecipitated CFTR and coimmunoprecipitated Hsc70 were quantified by densitometry, normalized, and denoted below the blots. Then, the relative amounts (the ratio of Hsc70/CFTR) were calculated and denoted in the top graph. The cellular expression levels of Hsc70 in the various experimental conditions were also compared by the western blots of lysates (5 μg), probed with anti-Hsc70 (the lower blot).

Figure 6: **Effect of PD98059 on the subcellular distribution of GFP-wt-CFTR in Cos7 cells exposed to butyrate.** Cos7 cells, transiently expressing GFP-wt-CFTR,

were observed 24 h after the addition of PD98059 (50 μM) and/or butyrate (5 mM). The subcellular distribution of GFP-wt-CFTR was directly visualized by the GFP fluorescence (right). The phase-contrast images were also revealed (left).

Figure 7: **Involvement of MAPK activity in CFTR expression.** (**A**) The effect of cotransfection of LA-SDSE-MAPKK (the left panel) and SASA-MAPKK (the right panel) on GFP-wt-CFTR expression was revealed by immunoblotting. Cos7 cells, cotransfected with the expression plasmids of GFP-wt-CFTR (1 μg) and either LA-SDSE-MAPKK (1 μg) or SASA-MAPKK (1 μg) were harvested 24 h after the addition of butyrate (5 mM). GFP-wt-CFTR expression was monitored using an anti-GFP antibody (the upper panel). The expression levels of either LA-SDSE-MAPKK or SASA-MAPKK (the middle panel), and the phosphorylated, active form of ERK/MAPK (the lower panel) were evaluated using anti-HA mAb and anti-phosphorylated ERK mAb. (**B**) The effect of cotransfection of LA-SDSE-MAPKK on GFP-ΔR-CFTR expression, revealed by immunoblotting. The expression levels of GFP-ΔR-CFTR, LA-SASE-MAPKK and phosphorylated ERK were detected as above. (**C**) Relative intensities of the C and B forms of GFP-wt-CFTR, monitored under cotransfection of LA-SDSE-MAPKK in the absence or presence of butyrate. The complex glycosylated C (white columns) and the core-glycosylated B (black columns) forms of GFP-wt-CFTR expressed in the cells were calculated from densitometry of immunoblots shown on (A). The amounts of the B and C forms with butyrate treatment were set to 1, and the relative amounts of those forms under cotransfection of LA-SDSE-MAPKK were quantified. The data are expressed as the mean $\pm$ SEM of three independent experiments. (**D**) Relative intensities of the C and B forms of GFP-ΔR-CFTR, monitored under cotransfection of LA-SDSE-MAPKK. The relative amounts of the C and B forms shown on (B) were quantified as above.

Figure 8: **Effect of LA-SDSE-MAPKK cotransfection on the subcellular**

Molecular Pharmacology Fast Forward. Published on August 10, 2004 as DOI: 10.1124/mol.104.001008
This article has not been copyedited and formatted. The final version may differ from this version.

distribution of CFTR. Cos7 cells were cotransfected with LA-SDSE-MAPKK and either GFP-wt-CFTR or GFP-ΔR-CFTR, and then incubated for 24 h in the absence (control) or presence of butyrate (5mM). The subcellular distribution of GFP-CFTR and GFP-ΔR-CFTR was directly visualized by the GFP fluorescence (middle). The subcellular distribution of LA-SDSE-MAPKK was visualized using an anti-HA antibody and a TRITC-labeled secondary antibody (right). DIC images were also revealed (left).

Molecular Pharmacology Fast Forward. Published on August 10, 2004 as DOI: 10.1124/mol.104.001008
This article has not been copyedited and formatted. The final version may differ from this version.

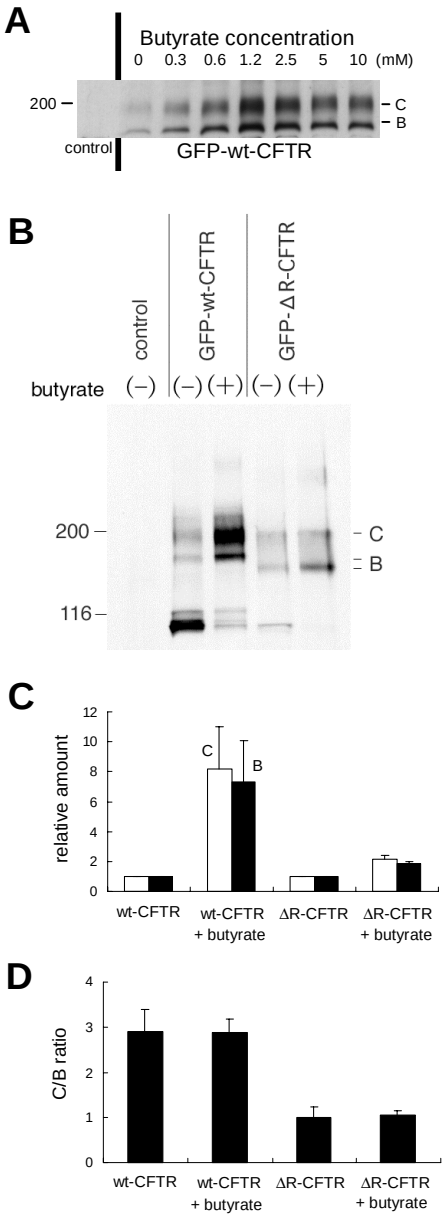

Figure 1

Molecular Pharmacology Fast Forward. Published on August 10, 2004 as DOI: 10.1124/mol.104.001008
This article has not been copyedited and formatted. The final version may differ from this version.

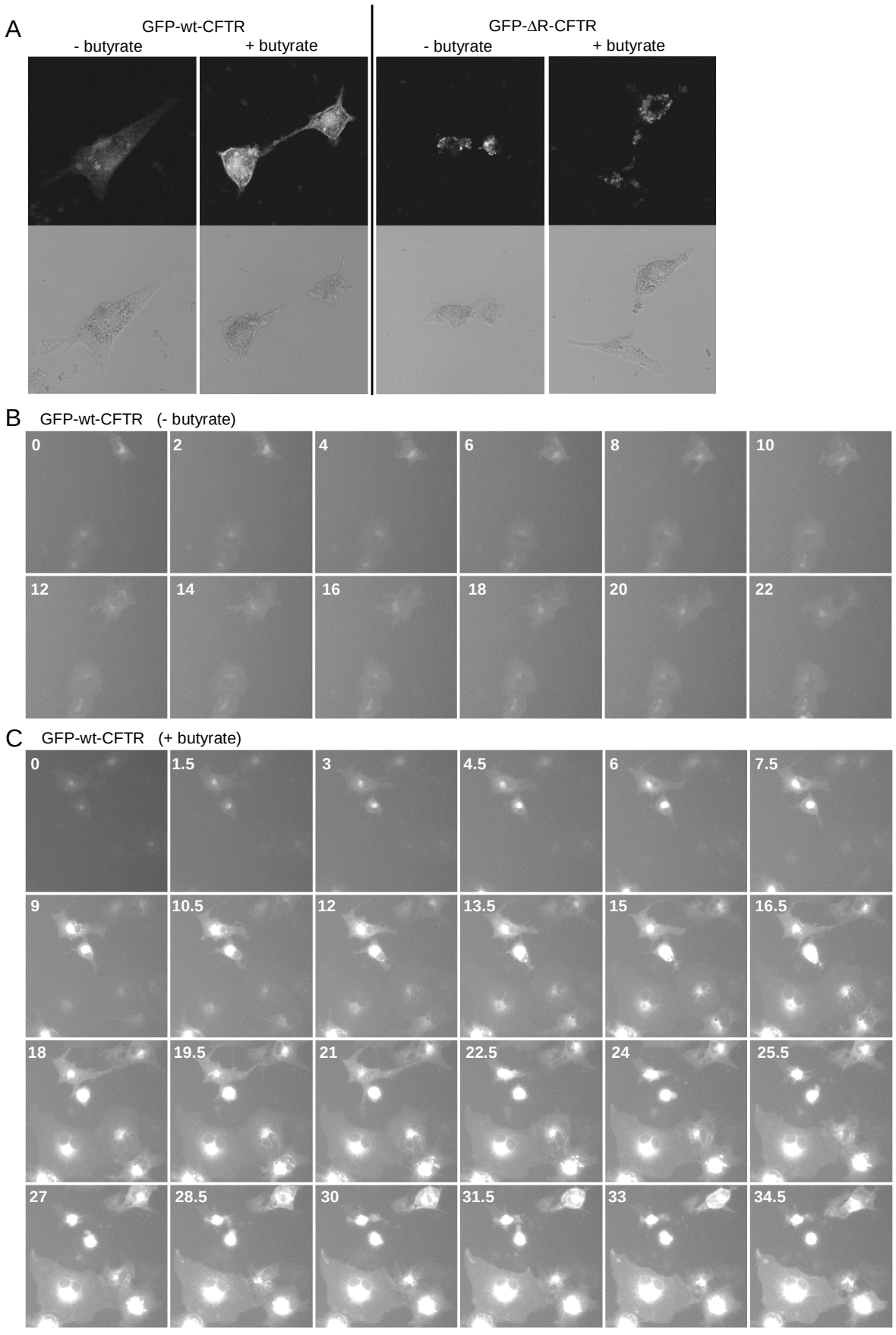

Figure 2

Molecular Pharmacology Fast Forward. Published on August 10, 2004 as DOI: 10.1124/mol.104.001008
This article has not been copyedited and formatted. The final version may differ from this version.

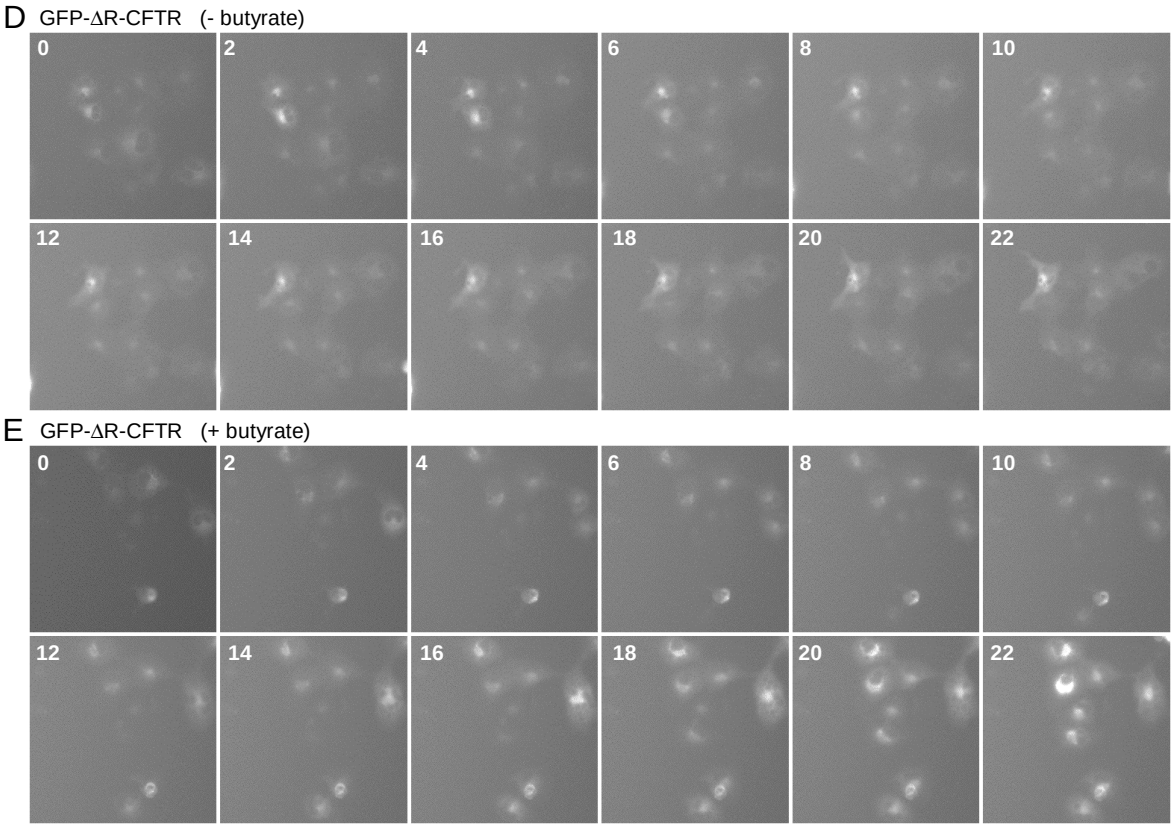

Figure 2

Molecular Pharmacology Fast Forward. Published on August 10, 2004 as DOI: 10.1124/mol.104.001008
This article has not been copyedited and formatted. The final version may differ from this version.

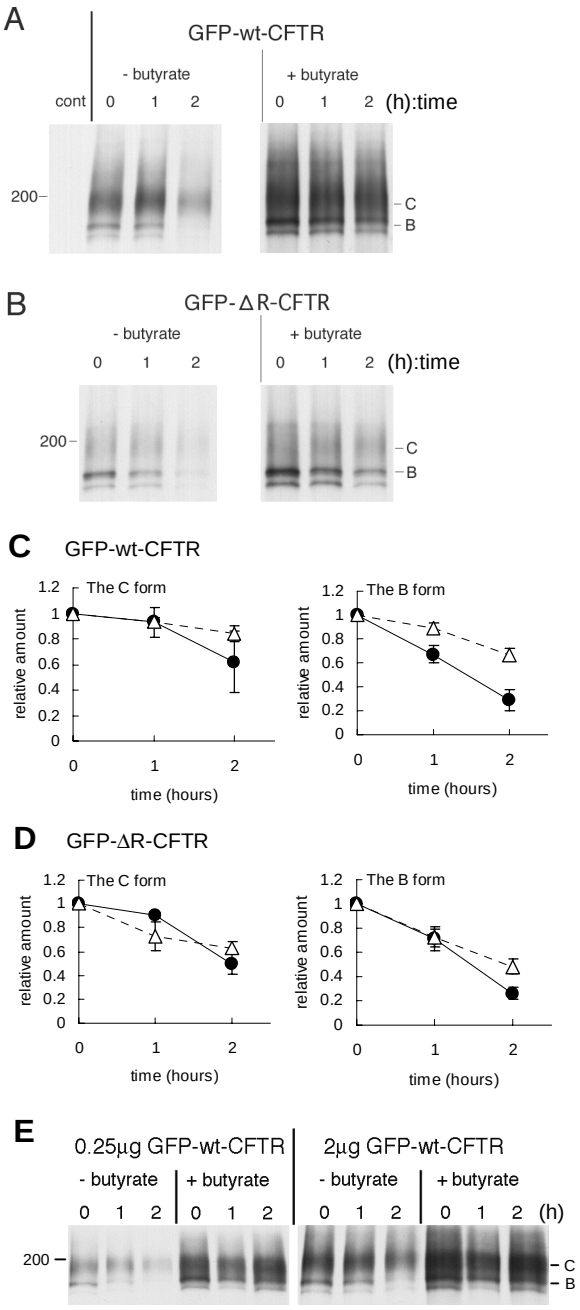

Figure 3

Molecular Pharmacology Fast Forward. Published on August 10, 2004 as DOI: 10.1124/mol.104.001008
This article has not been copyedited and formatted. The final version may differ from this version.

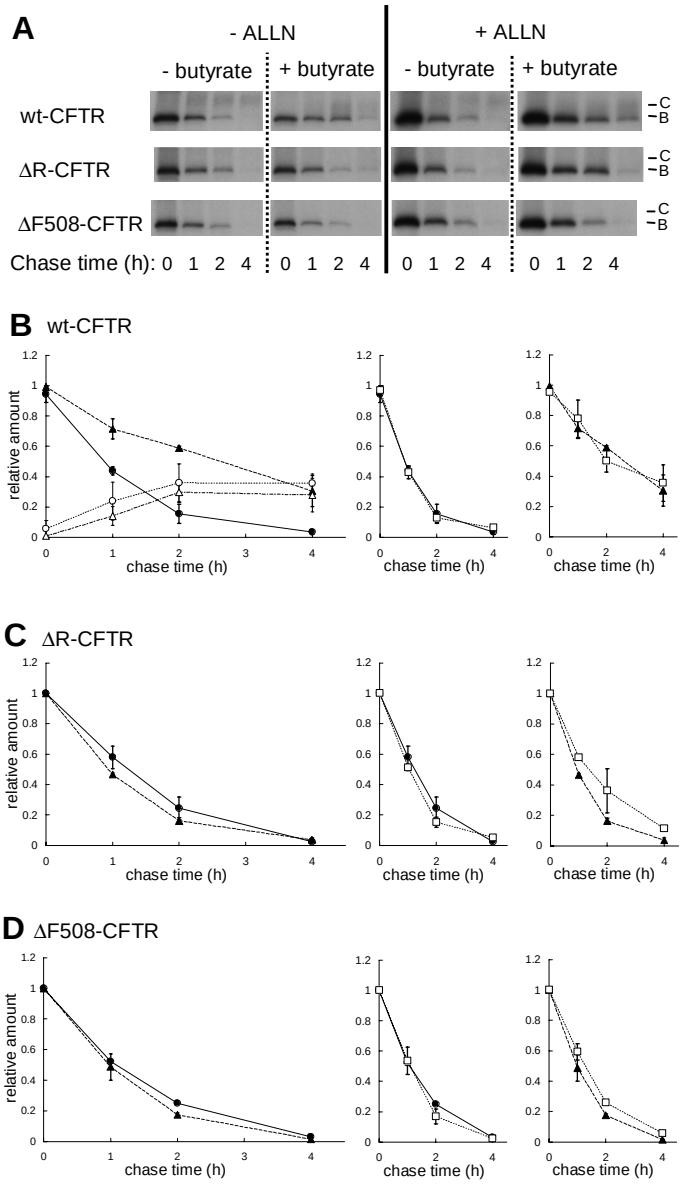

Figure 4

Molecular Pharmacology Fast Forward. Published on August 10, 2004 as DOI: 10.1124/mol.104.001008
This article has not been copyedited and formatted. The final version may differ from this version.

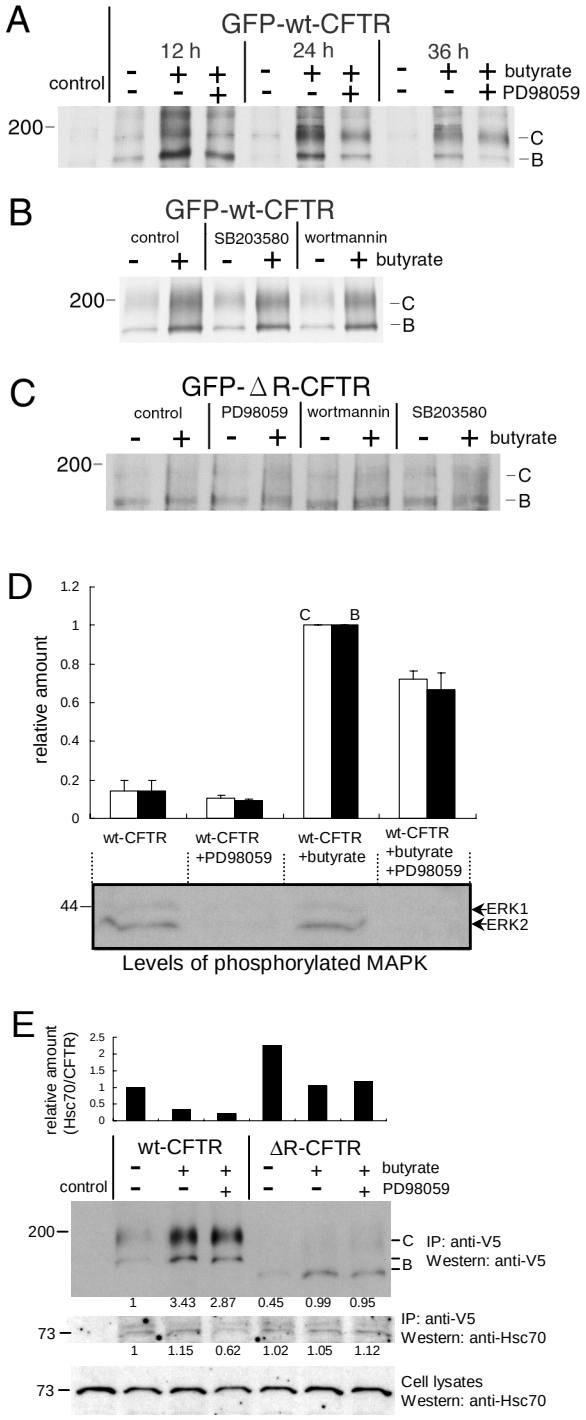

Figure 5

Molecular Pharmacology Fast Forward. Published on August 10, 2004 as DOI: 10.1124/mol.104.001008
This article has not been copyedited and formatted. The final version may differ from this version.

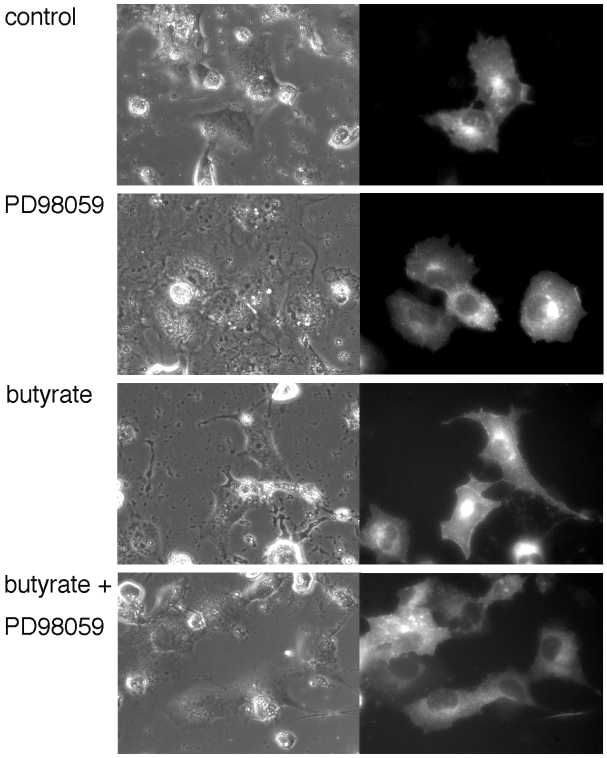

Figure 6

Molecular Pharmacology Fast Forward. Published on August 10, 2004 as DOI: 10.1124/mol.104.001008
This article has not been copyedited and formatted. The final version may differ from this version.

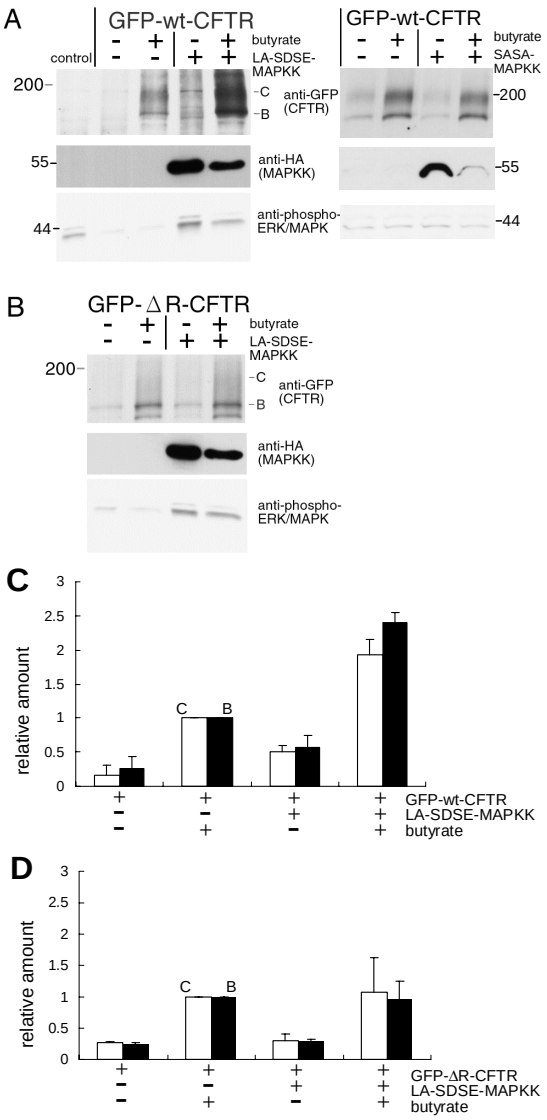

Figure 7

Molecular Pharmacology Fast Forward. Published on August 10, 2004 as DOI: 10.1124/mol.104.001008
This article has not been copyedited and formatted. The final version may differ from this version.

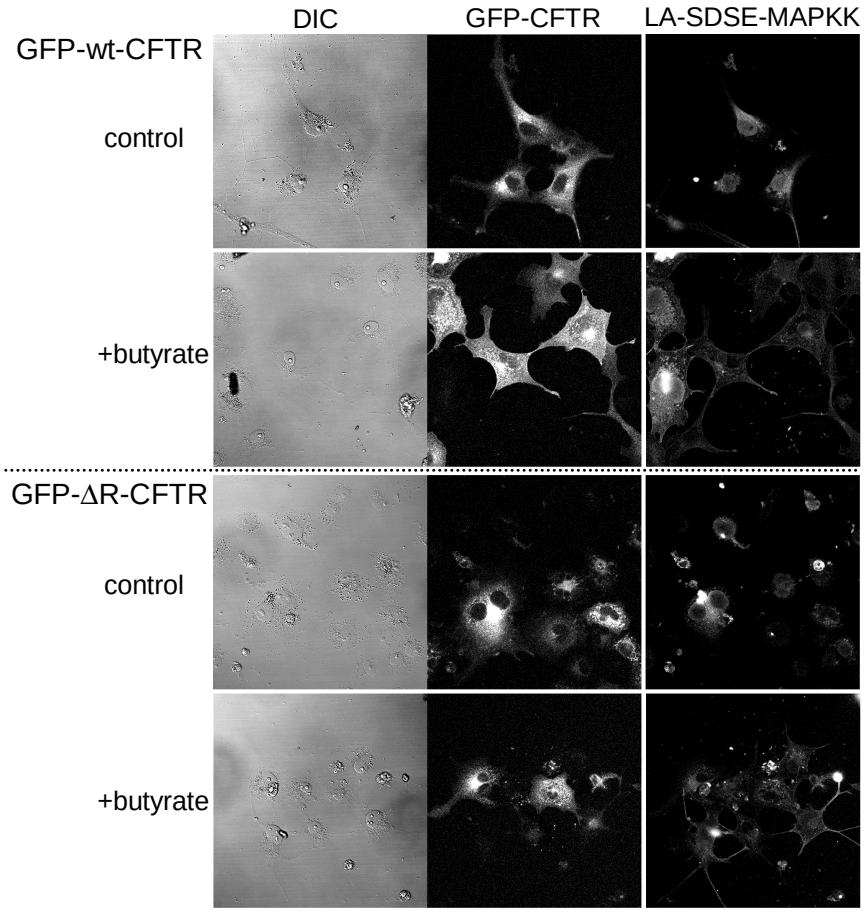

Figure 8